Carbohydrate Polymers 83 (2011) 1303–1310

Contents lists available at ScienceDirect

Carbohydrate Polymers

journal homepage: www.elsevier.com/locate/carbpol

Stability investigation of hyaluronic acid based nanoemulsion and its potential as transdermal carrier

Ming Kong, Hyun Jin Park*

Graduate School Biotechnology, Korea University, 1,5-Ka, Anam-Dong, Sungbuk-Ku, Seoul 136-701, South Korea

ARTICLE INFO

Article history:
Received 19 August 2010
Received in revised form 7 September 2010
Accepted 20 September 2010
Available online 29 September 2010

Keywords:
Hyaluronic acid
Nanoemulsion
Fluorescence
Stability
Encapsulation efficiency

ABSTRACT

In this study, stability of hyaluronic acid (HA) based nanoemulsion was systematically investigated. Factors including zeta potential, pH, crosslinking agents and degree of substitution (DS) were considered to assess their roles in stability. Nanoemulsions prepared from HA-GMS with higher DS showed smaller droplet sizes. In the presence of Ca^{2+} as a crosslinker, size distribution was improved to be more uniform at the expense of size increases within a controllable range. The optimal amount of Ca^{2+} usage was determined as 0.05%, which alleviated droplet flocculation and improved morphological qualities as well. Electrostatic, steric, and hydrophobic effects were verified to play crucial roles in emulsion stability. Surfactants strategy was another prerequisite making a key contribution. Encapsulation efficiency (E.E.) study using vitamin E as a model active ingredient proved the eligibility of HA-GMS nanoemulsion exploited as carriers, where the highest E.E. was 93.9 ± 1.4% occurring in sample L6. Fluorescence quenching assay offered evidence of VE encapsulation inside the hydrophobic interior of HA-GMS nanodroplets.

1. Introduction

With the advent of emulsion to achieve a mixture of two or more immiscible liquids, in which one liquid (the dispersed phase) is dispersed in the other (the continuous phase), the application fields of such colloidal objects (from nanomedicine, drug delivery and cosmetics, to food sciences) have become innumerable. Nano-emulsions are nanometric-sized emulsions and transparent or translucent systems, mainly covering a size range of 50–200 nm, and can be up to 500 nm. Nano-emulsions are also frequently known as miniemulsions, fine-dispersed emulsions, submicron emulsions and so forth, but are all characterized by great stability in suspension due to their very small size (Anton, Benoit, & Saulnier, 2008).

Unlike microemulsions, which are also transparent or translucent and thermodynamically stable (Overbeek, 1978), nanoemulsions are kinetically stable systems whose free energy of formation is greater than zero (Capek, 2004). However, the long-term physical stability of nanoemulsions makes them unique and they are sometimes referred to as 'approaching thermodynamic stability' (Tadros, Izquierd, Esquen, & Solans, 2004). Emulsion instability may occur by a number of different mechanisms, such as flocculation, creaming, coalescence and Ostwald ripening (http://en.wikipedia.org/wiki/Emulsion). Creaming and aggregation do not involve an increase in droplet size, but are precursors to coalescence, which along with Ostwald ripening directly induce droplet size growth. Emulsified droplets undergo a complexity of intrinsic and extrinsic forces, which are able to be classified into several interactive pairs, playing their specific roles individually or correlatedly in colloidal stability. Electrostatic interaction and steric forces are two primary factors to maintain emulsion stability. Both of which arise from interface features: electrostatic stabilization is based on the mutual repulsion of like electrical charges, steric forces between polymer-covered surfaces can modulate interparticle forces, producing an additional steric repulsive force (http://en.wikipedia.org/wiki/Colloid). As is the nature of emulsion, nanoemulsion exhibits classical behavior of metastable colloids, like Brownian motion, maintaining intrinsic droplet mobility. The nano-dimension renders van der Waals force, which is short-range and attractive force, to be considered as one instable factor. As particle size decreases, the rate of particles coalescence can increase since Brownian motion becomes more significant (Povey & Ding, 2010). In contrast to electrostatic interaction and steric force, Brownian motion and van der Waals forces are relatively weak, especially in the presence of an adsorbed layer at O/W interface rendering nanoemulsion kinetically stable (Capek, 2004). With regard to emulsion droplets, buoyance and gravitational force are two existing but negligible factors considering the tiny dimensions

* Corresponding author at: 1,5-Ka, Anam-dong, Sungbuk-ku, Green Campus, #307, Korea University, Seoul 136-701, South Korea. Tel.: +82 02 3290 4149; fax: +82 02 953 5892.
E-mail address: hjpark@korea.ac.kr (H.J. Park).

0144-8617/$ – see front matter © 2010 Elsevier Ltd. All rights reserved.
doi:10.1016/j.carbpol.2010.09.041

and primary interfacial effects of nanoemulsion. Besides these, emulsifiers' structure, like hydrophobicity, is another crucial factor concerning emulsion stability.

By virtue of their fine droplet diameter, larger surface area to volume ratio, and novel physicochemical properties like thermodynamical variability and transparent nature, the characteristics of nanoemulsions give them peculiar potentials to be applied in personal care products and cosmetics as well as in health care. Reasonable surfactant concentration, pleasant aesthetic character and skin feel are the outstanding advantages as compared with microemulsion (Tadros et al., 2004). Recently, there has been increased interest in the use of topical vehicle systems that could modify drug permeation through the skin. Many studies have shown that nanoemulsion formulations possess improved transdermal and dermal delivery properties, and have improved transdermal permeation of many drugs over the conventional topical formulations such as emulsions and gels (Shakeel et al., 2007).

Hyaluronan (hyaluronic acid, HA) is a sort of naturally occurring polymer, composed of unbranched repeating units of glucuronic acid and N-acetyl glucosamine linked by β1–3 and β1–4 glycosidic bonds (Ambrosio, Borzacchiello, Netti, & Nicolais, 1999). Properties of HA including specific viscoelasticity, biocompatibility, hydration and lubrication (Garg & Hales, 2004) make this polysaccharide potentially very useful in the food, medical and cosmetic industries. By means of HA based nanoemulsion, a promising transdermal carrier was developed in previous study, while products with improved stability and efficient function require further research.

In this study, stability and encapsulation investigations were conducted on HA based nanoemulsion we have developed. Several factors including droplet size, zeta-potential, hydrophobic character of amphiphilic HA, effect of pH and corsslinking agent were systematically assessed about their roles in nanoemulsion stability. Lipophilic vitamin E was selected as model active ingredient for evaluation of encapsulation efficiency.

2. Materials and methods

2.1. Materials

Sodium forms of HA with a molecular weight (MW) of 110 kDa and 10 kDa were a gift of Kolon Life Science, Korea. EDC and monostearin (glycerol α-monostearate, GMS) were purchased from Tokyo Kasei Kogyo Co., Ltd. (Japan). N-hydroxy succinimide (NHS, 97%) was acquired from Aldrich Chemical. Methylene chloride, potassium iodide, sodium thiosulfate pentahydrate, calcium chloride dehydrate and acetonitrile (HPLE grade) were purchased from Duksan Pure Chemical (Korea). Phosphate buffered saline (pH 7.4), α-tocopherol (97%), pyrene (98%) and cystamine dihydrochloride were purchased from Sigma–Aldrich. Various surfactants, polyoxyethylene sorbitan fatty acid esters (Tweens) and sorbitan fatty acid esters (Spans) were purchased from Samchun Pure Chemical (Korea). Uranyl acetate was offered by Electron Microscopy Sciences. Water, used for synthesis and characterization was purified by distillation, deionized and subjected to reverse osmosis using a Milli-Q Plus apparatus (Millipore, USA). All the chemicals were analytical grade and were used as received.

2.2. Synthesis of amphiphilic HA-GMS

Different batches of amphiphilic HA-GMS were synthesized by a previous method (Kong, Chen, & Park, 2010) (Table 1). Briefly, GMS was conjugated to HA by the formation of ester linkages through an EDC-mediated reaction. HA (190 mg) and EDC/NHS were dissolved in PBS at 1:1:1 mole ratio and maintained for 2 h. The solution was then added to GMS (60–540 mg) acetone solution dropwise with magnetic stirring. After a certain period of time, the resultant mixture was centrifuged. The apparent solution was extensively dialyzed and lyophilized. The structure of products was verified through FT/IR and degree of substitution of GMS was determined by ^{1}H NMR.

Table 1
The degree of substitution and yield of HA-GMS.

HA-GMS	HA (kDa)	DS (%)	Yield (%)
H6.5[a]	110	7	88.4
H14	110	14	88.1
H23	110	23	96.0
L6	10	6	93.2
L22	10	22	88.4

[a] Capitals denoted MW property of HA and numbers were DS of HA-GMS.

2.3. Preparation of HA-GMS nanoemulsions

Nanoemulsions were prepared through oil/water/surfactant (O/W/S) emulsifying system and solvent evaporation, using optimal conditions that have been screened. HA-GMS solution was the continuous phase, methylene chloride as oil phase, and Tween 80 and Span 20 (HLB = 12.5) as surfactants. The three components comprised in a mass ratio of 95/2/3. The disperse phase was added dropwise to a HA-GMS solution to form a coarse emulsion, which was further pulse-sonicated twice (pulse on, 10.0 s; pulse off, 2.0 s), using a Sonics Vibra-Cell CV33 ultrasonic probe (Sonics & Materials, USA) at 150 W in an ice bath for 3 min. The nanoemulsion obtained was crosslinked with or without $CaCl_2$ or cystamine (0.05, 0.10, and 0.20%, w/v), and then evaporated under reduced pressure for 30 min at room temperature to remove methylene chloride. Size analysis and zeta potential were determined on a Zetasizer ZEN 3600 Nano Series apparatus (ZEN, UK).

2.4. Fluorescence analysis

2.4.1. Self-assembling ability evaluation

Pyrene, used as a hydrophobic probe, was dissolved in ethanol at the concentration of 4.0 μg/mL. About 400 μL of this solution was pipetted into test tubes, and then the ethanol was driven off under reduced pressure. 4 mL ultrasonicated HA-GMS solutions, with series concentrations from 0.01 to 2 mg/mL, were added to the test tube, bringing the final concentration of pyrene to 2 μM. The mixture was incubated for 3 h in a water bath at 65 °C and shaken in a BS-10 skaking bed (Jeio Tech, Seoul, Korea) overnight at room temperature. Pyrene emission spectra were obtained using a Shimadzu RF-5301PC fluorescence spectrophotometer (Shimadzu Co., Kyoto, Japan). The probe was excited at 330 nm, and the emission spectrum was collected in the range of 350–500 nm at an integration time of 1.0 s. The excitation and emission slit opening were 10 and 3 nm, respectively.

2.4.2. Hydrophobic characteristic study of HA-GMS nanoemulsion

A similar method as mentioned above was used, except the analyte of interest was displaced by HA-GMS nanoemulsions at a concentration of 1 mg/mL, and crosslinked by Ca^{2+} (0.05%).

2.5. Effect of pH on nanoemulsion stability

Stability of HA-GMS nanoemulsion was evaluated through zeta potential measurement within pH range 4.0–8.0. The optical densities of nanoemulsion were determined simultaneously on Optizen 3220UV UV/vis spectrophotometer (Mecasys Co., Korea) at 600 nm (Chaix, Pacard, Elaïssari, Hilaire, & Pichot, 2003).

2.6. Methylene chloride residue detection

Methylene chloride residue was detected by gas chromatography (GC), a Hewlett Packard 5890 series II, 7376 controller (auto sampler) with data analysis by HP ChemStation software. The detector and column used were flame ionization detector (FID) and an HP-1 (crosslinked methyl siloxane) column (USA) with a 30 m × 0.2 mm × 0.25 mm film thickness. The injector and detector were operated at 200 °C and 220 °C, respectively, followed by a plateau at 280 °C for the cleaning of the column. The oven temperature was programmed to reach 150 °C at 10 °C/min. Single point internal standard was explored, using butonal as internal standard and 2% acetone solution as solvent. Nanoemulsion samples were mixed with solvent by vortex for 10 min. The mixtures were centrifuged at 25,000 × *g*, 4 °C for 30 min, and supernatants were added with butonal for GC determination.

2.7. Evaluation of active ingredient encapsulation efficiency (E.E.)

Vitamin E (α-tocopherol) was selected as model active ingredient for encapsulation study. Different amounts of VE were dissolved in methylene chloride before forming coarse emulsion. HA-GMS with different molecular weights and DS were prepared into nanoemulsion. The aqueous suspension was then eluted through a Sephadex G25 fine column to separate VE-encapsulated nanoparticles from free VE. Quantitative determination of encapsulated VE was achieved by HPLC using a reversed phase C18 column (Nova-Pak® C18, 3.9 mm × 150 mm, Waters Associates) operated at room temperature, a Waters 2690 Separation Module (Waters Associates) and a Waters 996 photodiode Array Detector (Waters Associates). Acetonitrile (HPLC grade) was used as eluent at a flow rate of 1 mL/min and chromatograms were analyzed with Waters Millennium 32 software. A calibration curve was constructed using the area under the curve (AUC) method and the total amount of VE was calculated by summing up all AUC. E.E. was calculated as the percentage of ratio of encapsulated VE mass to total VE mass.

2.8. Vitamin E fluorescence quenching assay

The quenching of VE fluorescence by I^- (KI) was monitored in solutions containing a 1.0×10^{-5} M antioxidant ($Na_2S_2O_3$). The fluorescence intensity of freshly prepared VE loaded HA-GMS nanoemulsions was acquired using Shimadzu RF-5301PC fluorescence spectrophotometer. VE was excited at 295 nm, and the emission spectrum was collected in the range of 300–410 nm at an integration time of 1.0 s. The excitation and emission slit opening were 3 and 3 nm, respectively (Hossu, Maria, Stoica, Ilie, & Iordan, 2009). All experiments were performed at room temperature. Collisional quenching of fluorescence is described by the Stern–Volmer equation:

$$\frac{I_0}{I_Q} = 1 + K_{SV}[Q] \quad (1)$$

where [Q] is the quencher concentration, K_{SV} is the dynamic quenching constant also called Stern–Volmer constant, and I_0 and I_Q are the fluorescence intensities in the absence and presence of quencher, respectively.

2.9. Transmission electron microscopy (TEM)

Specimens were prepared by dropping sample solution onto a carbon-coated copper grid. The grid was held horizontally to allow the molecular aggregates to settle, and then held at a certain angle to allow excess fluid to drain onto filter paper. One drop of 2% uranyl acetate was added on the horizontal grid to give a negative staining. The specimens were allowed to air-dry prior to TEM examination using Tecnai G2 F30 microscope (Philips-FEI, Holland). TEM studies were conducted at KBSI (Seoul).

2.10. Statistical analysis

The assays were performed at least in triplicate. The data collected in this study are expressed as the mean ± standard deviation.

3. Results and discussions

3.1. Characteristics of HA-GMS

Amphiphile HA-GMS was synthesized through esterification between carboxyl groups on HA molecular chains and hydroxyl groups from GMS. The chemical structures of HA-GMSs were verified by FT/IR, and degrees of substitution were determined by ^{1}H NMR (Table 1). Different batches of HA-GMSs were prepared differing from molecular weight (Mw) and degree of substitution (DS). A higher DS demonstrated a larger amount of GMS was conjugated on the HA molecules, giving stronger hydrophobicity to the obtained HA-GMS.

The self-assembling ability of HA-GMS was evaluated by fluorescent emission spectrum within the range of 330–500 nm, and H6.5 was chosen for evaluation. The H6.5 solution was ultrasonicated directly without any surfactants or oil phase. The peak 384/372 ratio of pyrene can be used to determine the reactivity or assembling properties of amphiphilic molecules to the change in environment hydrophobicity in the aqueous system (Chen, Lee, & Park, 2003). The peak 384/372 ratios at series concentrations of the HA-GMS emulsions are shown in Fig. 1. The peak 384/372 ratio began to increase from 0.25 mg/mL and this trend continued on. The increase in the peak 384/372 ratio indicates the development of a hydrophobic environment resulting from the occurrence of self-assembly under ultasonication. For the other samples (H14, H23, L6 and L22), higher DS gave them stronger hydrophobic effects facilitating their molecular self-assembly (data not shown). For L6, the shorter molecular chain length imparted relatively higher hydrophobic effect compared with H6.5. 1.0 mg/mL was accordingly selected as the concentration for further nanoemulsion studies.

3.2. Characterizations and stability investigations of HA-GMS nanoemulsions

3.2.1. Droplet size analysis

The mean size and polydispersity index (PdI) of the HA-GMS nanoemulsions were measured shortly after preparations. As

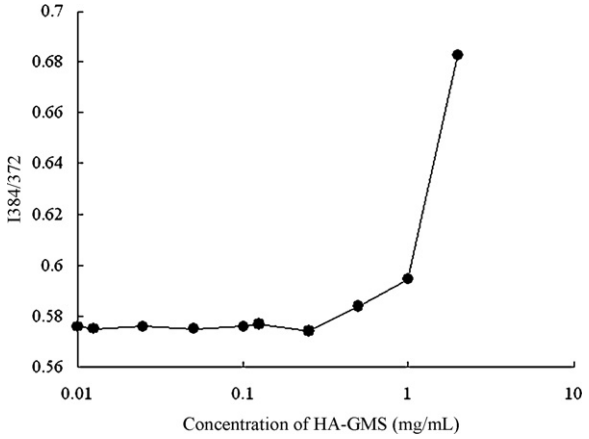

Fig. 1. Peak 384/372 ratio of pyrene fluorescence as a functional of HA-GMS (H6.5) concentration in emulsion without surfactants. H6.5 denotes high Mw HA-GMS with DS of 6.5%.

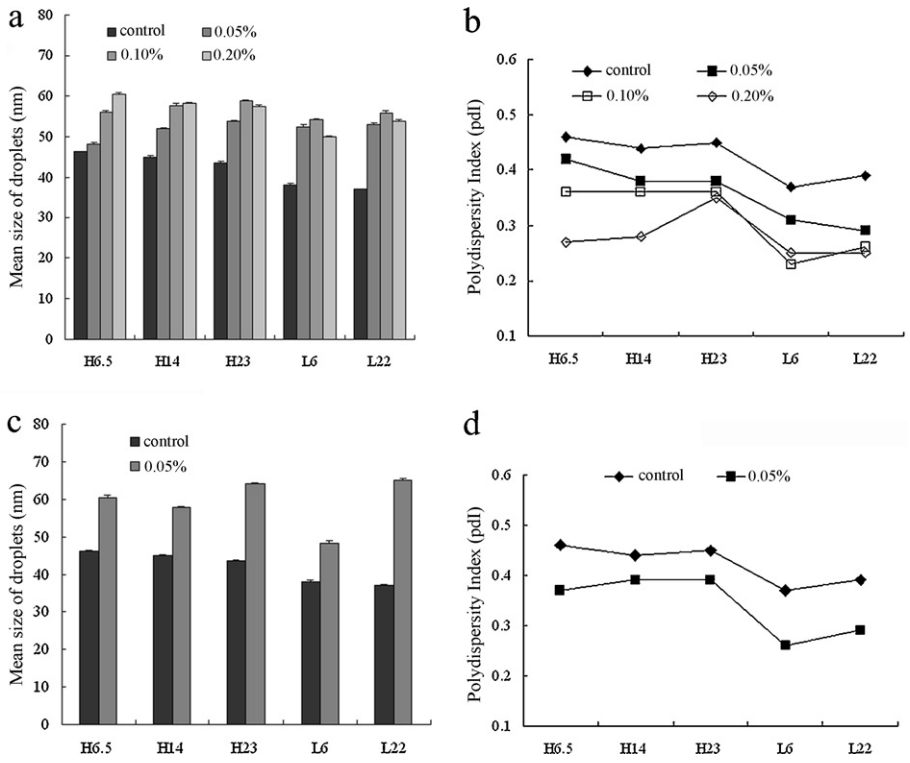

Fig. 2. Droplet size and polydispersity index (PdI) of HA-GMS nanoemulsions (1.0 mg/mL) as functions of $CaCl_2$ concentrations: (a) mean size of droplets; (b) PdI; and as functions of cystamine dihydrochloride concentrations: (c) mean size of droplets; (d) PdI. H6.5, H14, H23, L6 and L22, where capitals denote MW property of HA and the latter numbers are DS of HA-GMS.

shown in Fig. 2a, the control groups treated without Ca^{2+} displayed declines in mean size from H6.5 to L22 consecutively. For samples with identical HA Mw, size reduction accompanied an increase of DS, coinciding with our previous study (Kong et al., 2010). The size variations demonstrated that the nanoemulsified droplet sizes closely correlated to the amphiphiles' hydrophobicity and higher DS gave stronger hydrophobicity leading to smaller sizes. Nevertheless, relatively more pronounced reduction was observed for high Mw, from 46.2 to 43.6 nm, than for low Mw, from 38.1 to 37.1 nm. These differences might have come from differing molecular chain lengths. Shorter chain lengths might have imparted HA-GMS of similar DSs with relatively stronger hydrophobic effects, which generated more compact droplets. The smaller mean sizes of low Mw samples support this speculation. The size distribution indicated by PdI is shown in Fig. 2b. PdI maintained at a relatively high level from 0.46 to 0.39, demonstrating a relatively wide size distribution. In our previous study, instability was found concerning flocculation generation during storage, thereinto, a wide size distribution probably played certain effect. Further study regarding instability factors were made to improve nanoemulsion qualities.

3.2.2. *Effect of crosslinking agents*

HA is usually considered as anionic polysaccharide and has a very low isoelectric point about 2.5 (Gatej, Popa, & Rinaudo, 2005). The carboxyl groups are desirable substrate to be crosslinked, through which nanoparticles have actually been prepared with calcium ions as crosslinker (Shi, Du, Yang, Zhang, & Sun, 2005). Inorganic and organic crosslinkers were considered, Ca^{2+} was divalent while cystamine, having two primary amines linked by a disulfide linkage, conjugated to carboxylic acid groups in HA (Lee, Jeong, & Park, 2007).

The HA-GMS nanoemulsions (1 mg/mL) were treated with different amount of crosslinker. 0.05–0.2% calcium chloride dehydrate solution (mole ratio of $-COO^-/Ca^{2+}$ ranged from 3.7 to 14.7) and 0.05% cystamine dihydrochloride solution (mole ratio of $-COO^-/Ca^{2+}$ equals to 22.7) were added to the nanoemulsions right after sonication, respectively. Varying extents of droplet size increases were found after crosslinking treatments (Fig. 2). For Ca^{2+}, the size rising trend generally boosted as the concentration of crosslinker increased, such as mean size of H6.5 changed from 46.2 nm to 60.4 nm with a rising ratio of 30.8%, while the ratio for L22 was the highest at 50.9% (Fig. 2a). Calcium ions are known as a factor that may lead to macromolecule aggregates in vitro and in vivo, such as globulin, lipids and vesicles. This property within proper amount of calcium ions may bring local but not large scale accumulations of HA molecular chains, and cause finite increase of surface thickness other than aggregations. Accumulations like these are desirable owing to their strengthening surface rigidness and burying of functional groups inside, which consequently reduce interfacial reactions and enhance nanoemulsion stability. These desirable accumulations are able to avoid existence of very small droplets as well, which can be captured by larger ones. This presumption was confirmed by decreasing PdI in the presence of Ca^{2+} (Fig. 2b), indicating corsslinked droplets distributed in a narrower range. Therefore, the key is to figure out the proper amount of Ca^{2+}. Considering the principle of our nanoemulison preparation was to acquire a small size emulsion applicable as transdermal carriers, 0.05% was chosen as the desirable amount of crosslinking agent. This amount did not change droplet sizes much and improve size distribution as well. In the case of cystamine, the same phenomena were found (Fig. 2c and d), otherwise, the treated mean droplet sizes were so large with just under 0.05% that they were beyond the criterion. The pronounced changes probably arise from their lager molecular size other than calcium ions.

3.2.3. *Effect of hydrophobicity*

Size variations with DS were presumed to associate with hydrophobic effects of HA-GMSs. Hydrophobic studies of HA-GMSs

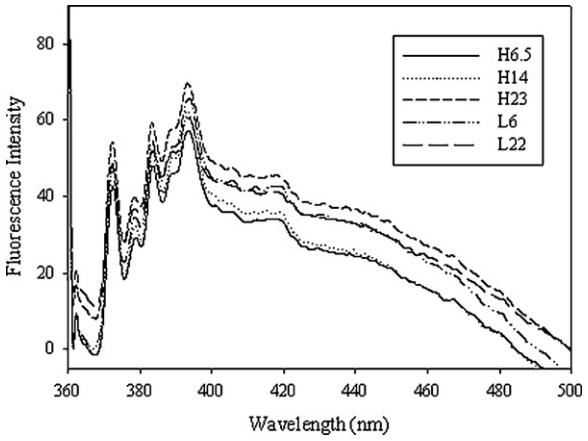

Fig. 3. Pyrene fluorescence intensity of HA-GMS nanoemulsions (1.0 mg/mL). H6.5, H14, H23, L6 and L22, where capitals denote MW property of HA and the latter numbers are DS of HA-GMS.

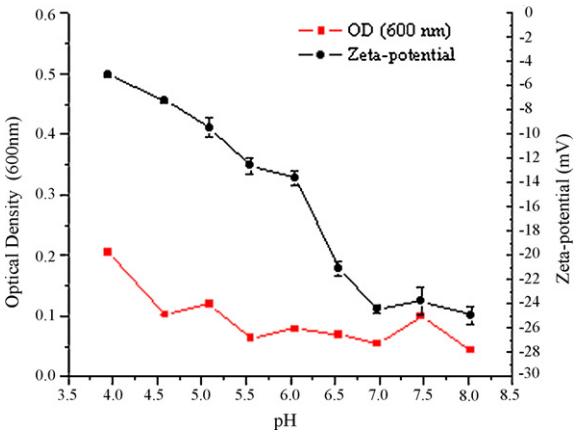

Fig. 4. Correlation between optical density at 600 nm and zeta potential of HA-GMS nanoemulsion (H6.5, 1.0 mg/mL) as function of pH.

through fluorescence offered evidence to this presumption (Fig. 3). The spectra of either sample loaded with pyrene as hydrophobic probe displayed different intensities from each other, especially at specific peaks 372, 383 and 393 nm. The fluorescence intensities positively correspond to the hydrophobicity of sample. Although the hydrophobic differences were slight, they led to differing performances on droplet size. For samples with identical Mw, the spectra arrays from top to bottom coincided with the DS decline. These were H23, H14 and H6.5 for high Mw, and L22 and L6 for low Mw. Meanwhile, the low Mw samples showed higher intensities than the high Mw ones. From the fluorescence intensity distribution, the hydrophobic effects of the treated samples from strong to weak were L22, L6, H23, H14 and H6.5. Samples of higher DS within identical Mw and lower Mw exhibited stronger hydrophobic effects, which verified the postulation mentioned in size analysis. Hydrophobic effect was suggested to play a crucial effect in improving nanoemulsified droplet size distributions, and thus, stabilize the system.

3.2.4. Effects of zeta potential and pH

The most important factor that affects zeta potential is pH. A zeta potential value on its own without a quoted pH is a virtually meaningless number (Zetasizer Nano Series User Manual, 2004). Zeta potential was investigated as a function of pH in order to reveal the effect of pH on net surface charge density variation (Fig. 4). The nanoemulsion prepared with H6.5 and crosslinked by Ca^{2+} in deionized water underwent pH adjustments from 4.0 to 8.0, and turbidities of nanoemulsions were assessed via optical density at 600 nm. Absolute zeta potential increased as ambient pH varied from acid to alkaline and leveled off around 25 mV. On the other hand, corresponding turbidities tended to rise under low zeta potentials. At the acidic end, the nanoemulsion was highly hazy, with OD_{600} nm around 0.205. The native pH of freshly prepared nanoemulsion was around 5.5 due to HA's weak acidity with a zeta potential of −12.57 mV. The negative charges derived from two sources, one was carboxylic groups as detecting pH was below HA's isoelectric point (p*I* = 2.5), and another was the so-called "non-ionic" surfactant Span. Span is actually an ionic surfactant in non-polar low conducting media, probably attributed to dissociation of span molecules or their stabilization of ions originally existing in the liquid as neutral ion pairs (Dukhin & Goetz, 2004). The negative charges supplied electrostatic repulsion among droplets.

As another major effect on nanoemulsion stability, electrostatic effect is a key factor must be considered. It has been suggested that zeta potential may serve as a partial indicator for the physical stability of the emulsion being formed. High absolute zeta potential values (above 30 mV) should preferably be achieved in most emulsions prepared in order to ensure the creation of a high-energy barrier against coalescence of the dispersed droplets (Zhao et al., 2010). However, this suggested zeta potential cut-off point is only an experience-based value and cannot be reliably used to predict the stability of nanoemulsion. In the HA-GMS nanoemulsions, the smaller droplet size compared with the reports may fill the gaps between its zeta potential and the empirical value. Moreover, under neutral condition, zeta potentials were close to the empirical value.

3.2.5. Other considerations

Our previous study evaluated the size variation over 96 h in storage and found size reduction without size aggregates (Kong et al., 2010). In this study, size variations occurred counting on series of events (Table 2). The naked emulsified droplet size (HA free) increased throughout with treatments of HA-GMS addition (L6 as sample), HA-GMS concentration, crosslinking agent and VE loading. Sizes were also found to decrease after 15 d storage. Size reduction ratio calculated by size changing percentages showed similar

Table 2
Size variations along with series of events.

	Initial		15 d		Size reduction ratio $100 \times (Dt - Di)/Di$
	Di[a]: size (nm)	PdI	*Dt*[a]: size (nm)	PdI	
HA free NE	38.1 ± 0.1	0.577	29.1 ± 0.3	0.469	24
HA NE					
1.0 mg/mL	48.4 ± 0.4	0.41	42.2 ± 0.3	0.35	13
2.0 mg/mL	54.3 ± 0.2	0.37	50.0 ± 0.1	0.33	8
NE[b] + Ca^{2+} (0.05 mg/mL)	51.4 ± 0.1	0.24	44.7 ± 0.2	0.24	13
VE (1 mg/mL) loading NE[b] + Ca^{2+}	56.9 ± 0.4	0.26	48.9 ± 0.4	0.28	14

[a] *Dt* is droplet diameter at time *t* and *Di* is the initial droplet diameter.
[b] The emulsions were prepared of 1.0 mg/mL HA-GMS (L6).

value around 13% for emulsions containing 1.0 mg/mL HA-GMS, suggesting constant structure changes. The size reduction probably arose from solvent evaporation leading to re-arrangement of surface molecules. The flocculation generated on the bottom in previous study was alleviated to a much larger extent in this study with aid of crosslinking agents. Perfect solution to this instability problem seems theoretically impossible ascribing from the instinctive thermal-variability of nanoemulsion.

There remains another non-negligible effect, namely steric forces introduced by surfactants, which also provided steric repulsion to stabilize emulsion against coalescence (Capek, 2004). Furthermore, the non-ionic surfactant mixture in this study was able to attain better performance than those attainable with the individual components by themselves (Rosen, 2004).

3.3. Methylene chloride residue detection

Methylene chloride is the least toxic of the simple chlorohydrocarbons, but it is not without its health risks as its high volatility makes it an acute inhalation hazard (Rioux & Myers, 1988). Toxicity assessments therefore become necessary in practical application. 1-Butonal (b.p. 117.5 °C) was utilized as an internal standard and 2% acetone solution as the solvent in GC detection. Initially, 10 mg/mL methylene chloride and butonal dissolved in solvent were detected to figure out the internal response factor and the retention time of methylene chloride. For nanoemulsion samples, solvent was mixed with samples by volume ratio of 1:1 to extract methylene chloride residue. The extractions were then separated from the droplets by centrifuge. The theoretical amount of methylene chloride in the nanomulsion was 20 mg/mL prior to its evaporation. In order to detect the possible residue of methylene chloride, different amounts of butonal, including 10, 20 and 30 mg/mL were, respectively, added into analytes to obtain different degrees of sensitivities. No peaks were identified at methylene chloride's retention time on determined spectra for all samples, suggesting no residue remained in the final products of the nanoemulsions. This result guarantees the security of nanoemulsions absent from methylene choride.

3.4. E.E. of active ingredient

With the purpose to develop a carrier for active ingredient, vitamin E (VE) was selected as model component to evaluate E.E.s of the HA-GMS nanoemulsions. Samples prepared from different Mw and DS, H6.5, H23 and L6 were chosen for VE loading (1.0 mg/mL). As shown in Fig. 5a, E.E.s of the three samples varied from each other and increased with the order of H6.5, H23 and L6, from 53.49% to 93.89%. The variances among samples are mainly attributable to the hydrophobic effects, which strengthened in the same order with E.E.s. Since VE is totally hydrophobic that only present in the hydrophobic inner parts of droplets, samples with stronger hydrophobicity have larger potential to hold VE inside. These variances have almost nothing to do with the droplet size, because no significant size differences have been found among samples crosslinked with Ca^{2+}. However, VE loading definitely rendered size increments in either sample (data not shown).

The E.E.s were also discovered to be VE concentrations dependent (Fig. 5a). As VE concentration increased from 0.5 mg/mL to 1.0 mg/mL, E.E.s decreased among the samples, especially for H6.5, varying from 92.21% to 53.49%. At the concentration of 0.5 mg/mL, every sample showed high E.E.s. The dependence upon VE concentration can be explained by VE saturation process. At low concentration, VE is able to be completely entrapped in the void spaces of nanoemulsified droplets. With the growth of VE amount, the void spaces would be filled, described as saturation, and the droplets would not encapsulate any more VE. Thereafter, if concentration kept increasing, the additional amount of VE would be expelled out of droplets and run free in the continuous phases, leading to decreases of E.E.s.

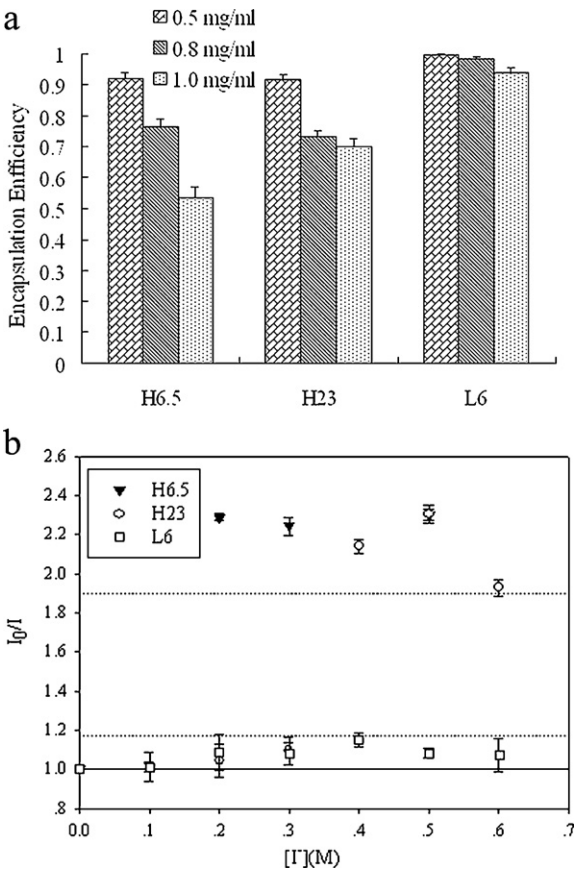

Fig. 5. (a) Encapsulation efficiency of vitamin E loaded HA-GMS nanoemulsions (1.0 mg/mL) as function of VE concentration; (b) fluorescence quenching of VE loaded HA-GMS nanoemulsions (1.0 mg/mL) as function of concentration of quenching agent potassium iodide. H6.5, H23 and L6, where capitals denote MW property of HA and the latter numbers are DS of HA-GMS.

3.5. Fluorescence quenching assay

In order to further verify the encapsulation of VE inside emulsified HA-GMS droplets, spectroscopic methods were utilized to detect and measure the changes in microscopic levels. Fluorescence quenching is a suitable technique for providing information on the location of α-Toc (VE) in micellar and lipid systems, mainly due to fluorescence spectrum sensitivity to microenvironment (Dwiecki, Górnas, Wilk, Nogala-Kałucka, & Polewski, 2007). According to fluorescence emission spectra (300–410 nm), VE exhibited fluorescence with a maximum at 323 nm as encapsulated in the HA-GMS nanoemulsion. Large, hydrated, I^- ions, used as quenching agents, are not able to penetrate into hydrophobic regions, limiting their quenching activity to DOX molecules in the hydrophilic region and the interface (Missirlis, Kawamura, Tirelli, & Hubbell, 2006). The slopes of Stern–Volmer plots for encapsulated VE (Fig. 5b) reflect the degree of exposure to the quenching I^-. Unlike the reported plots those were linear profiles (Dwiecki et al., 2007; Missirlis et al., 2006), owing to different formulation of carriers from the literatures, the slopes were not constant in this experiment. For H6.5, fluorescence was quenched soon as I^- concentration rose to 0.2 M. Similar case occurred at concentration 0.4 M for H23 but was not observed for L6, upon which I^- had no effects. VE fluorescence quenching is available only via collision between its chromophore and I^- (Dwiecki et al., 2007), which is accordingly accessible for the

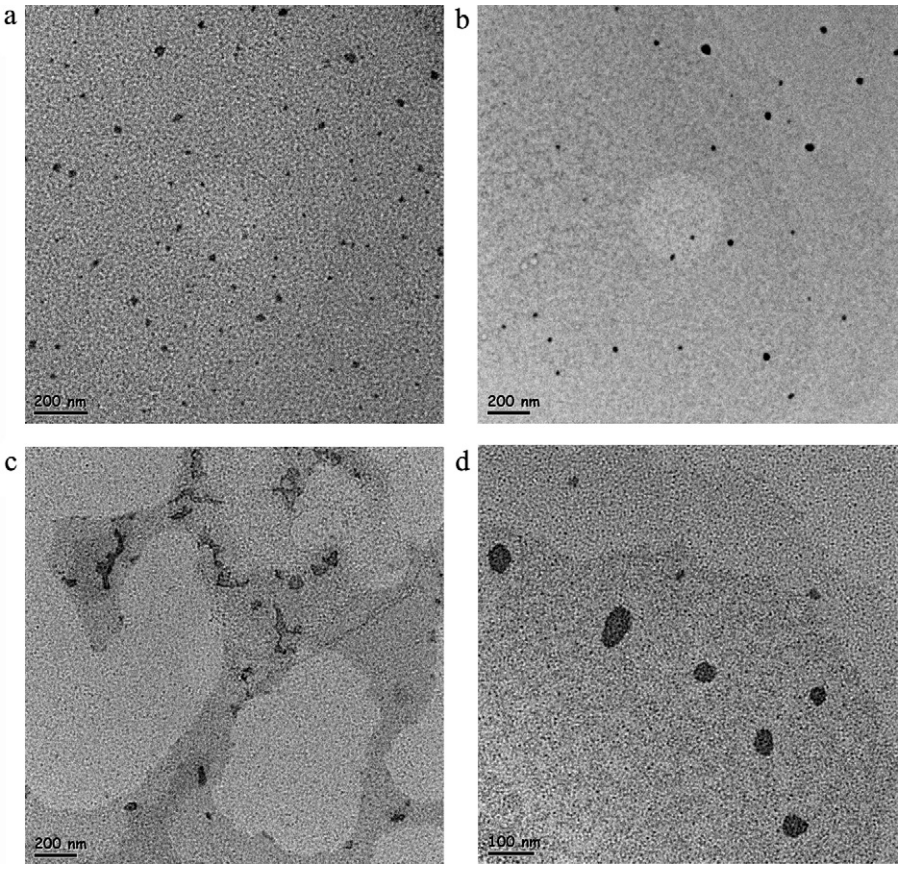

Fig. 6. TEM morphological observation of HA-GMS nanoemulsion (L6): (a) HA-GMS nanoemulsion (1.0 mg/mL); (b) HA-GMS nanoemulsion (1.0 mg/mL) crosslinked with Ca^{2+} (0.05%); (c) HA-GMS nanoemulsion (1.0 mg/mL) loaded with VE (1.0 mg/mL); (d) HA-GMS nanoemulsion (1.0 mg/mL) loaded with VE (1.0 mg/mL) and crosslinked with Ca^{2+}(0.05%).

free VE outside the emulsified droplets. Based on this theory, the results obtained through fluorescence quenching agree with the E.E. study: H6.5 with the lowest E.E. had the largest amount of free VE capable of being quenched, and L6 had limited amount of free VE resulting in no significant quenching outcome. The results meanwhile verify the encapsulated VE located inside the hydrophobic interior of HA-GMS nanodroplets.

3.6. TEM observation

Because of better performance of L6 nanoemulsion in terms of size distribution and E.E., it was taken as specimen for TEM morphological observation. L6 nanoemulsions (1.0 mg/mL) treated with or without Ca^{2+}, and VE free or loading, were considered for comparison (Fig. 6). L6 droplets without crosslinking exhibited various sizes and irregular morphology (Fig. 6a), Ca^{2+} gave more uniform size distribution and spherical appearances (Fig. 6b). Fig. 6c displays VE loaded droplets absent of Ca^{2+}, and aggregates of droplets are readily identified. In contrast, crosslinking agents stabilized the droplets are free of aggregates and increased the droplet size concomitantly (Fig. 6d). Morphological observations provide direct evidence to crosslinking effect and size variation as discussed above.

4. Conclusion

HA-GMS nanoemulsions offer an ideal starting point for the development of colloidal carriers for active ingredients with small sizes and are capable for transdermal applications. In particular, nanoemulsion stability was studied systematically and improved through crosslinking agent, adjusting pH and controlling DS of HA-GMS. Among the factors considered, electrostatic, steric and hydrophobic effects play key roles in stability. Additionally, surfactant molecules are crucial modulator to stabilize colloidal interface meanwhile favor to downsize droplets. Encapsulation efficiency investigations demonstrate that HA-GMS nanoemulsions are qualifiable carriers for lipophilic ingredients. Targeting application as transdermal carrier, further studies regarding skin permeability and bioavailability assessments will be performed in our following researches. The small size, improved stability, and desirable performances make HA-GMS nanoemulsion a potentially interesting colloidal transdermal carrier for skin care and cosmetic products.

Acknowledgement

This study was supported by a Grant of the Korea Health 21 R&D Project, Ministry of Health and Welfare, Republic of Korea (A050376).

References

Ambrosio, L., Borzacchiello, A., Netti, P. A., & Nicolais, L. (1999). Rheological study on hyaluronic acid and its derivative solutions. *Journal of Macromolecular Science, Part A*, *36*, 991–1000.

Anton, N., Benoit, J. P., & Saulnier, P. (2008). Design and production of nanoparticles formulated from nano-emulsion templates—A review. *Journal of Controlled Release*, *128*, 185–199.

Capek, I. (2004). Degradation of kinetically-stable o/w emulsions. *Advances in Colloid and Interface Science*, *107*, 125–155.

Chaix, C., Pacard, E., Elaïssari, A., Hilaire, J. F., & Pichot, F. (2003). Surface functionalization of oil-in-water nanoemulsion with a reactive copolymer: Colloidal characterization and peptide immobilization. *Colloids and Surfaces B: Biointerfaces*, *29*, 39–52.

Chen, X. G., Lee, C. M., & Park, H. J. (2003). O/W emulsification for the self-aggregation and nanoparticle formation of linoleic acids modified chitosan in the aqueous system. *Journal of Agricultural and Food Chemistry*, *5*, 3135–3139.

Dukhin, A. S., & Goetz, P. J. (2004). *Ionic properties of so-called "non-ionic" surfactants in non-polar liquids*. Bedford Hills, NY, USA: Dispersion Technology, Inc.

Dwiecki, K., Górnas, P., Wilk, A., Nogala-Kałucka, M., & Polewski, K. (2007). Spectroscopic studies of D-α-tocopherol concentration-induced transformation in egg phosphatidylcholine vesicles. *Cellular and Molecular Biology Letters*, *12*, 51–69.

Garg, H. G., & Hales, C. A. (2004). *Chemistry and biology of hyaluronan*. London: Elsevier Science & Technology Books.

Gatej, I., Popa, M., & Rinaudo, M. (2005). Role of the pH on hyaluronan behavior in aqueous solution. *Biomacromolecules*, *6*, 61–67.

Hossu, A. M., Maria, M. F., Stoica, A., Ilie, M., & Iordan, M. (2009). Determination of tocopherol in oil pharmaceuticals by using the spectrofluorimetry and method validation. *Ovidius University Annals of Chemistry*, *20*, 53–56.

Kong, M., Chen, X. G., & Park, H. J. (2010). Design and investigation of nanoemulsified carrier based on amphiphile-modified hyaluronic acid. *Carbohydreate Polymers,* doi:10.1016/j.carbpol.2010.08.001.

Lee, H. J., Jeong, Y. H., & Park, T. G. (2007). Shell cross-linked hyaluronic acid/polylysine layer-by-layer polyelectrolyte microcapsules prepared by removal of reducible hyaluronic acid microgel cores. *Biomacromolecules*, *8*, 3705–3711.

Missirlis, D., Kawamura, R., Tirelli, N., & Hubbell, J. A. (2006). Doxorubicin encapsulation and diffusional release from stable, polymeric, hydrogel nanoparticles. *European Journal of Pharmaceutical Sciences*, *29*, 120–129.

Overbeek, J. T. G. (1978). The first rideal lecture: Microemulsions, a field at the border between lyophobic and lyophilic colloids. *Faraday Discussions of the Chemical Society*, *65*, 7–19.

Povey, M., & Ding, Y. L. (2010). *Nanodispersion and method of formation thereof*. WO/2010/038087

Rioux, J. P., & Myers, R. A. (1988). Methylene chloride poisoning: A paradigmatic review. *The Journal of Emergency Medicine*, *6*, 227–238.

Rosen, M. J. (2004). *Surfactants and interfacial phenomena* (3rd ed.). New Jersey: John Wiley & Sons, Inc. (Chapter 11).

Shakeel, F., Baboota, S., Ahuja, A., Ali, J., Aqil, M., & Shafiq, K. (2007). Nanoemulsions as vehicles for transdermal delivery of aceclofenac. *AAPS PharmSciTech*, *8*, 191–199.

Shi, X., Du, Y., Yang, J., Zhang, B., & Sun, L. (2005). Effect of degree of substitution and molecular weight of carboxymethyl chitosan nanoparticles on doxorubicin delivery. *Journal of Applied Polymer Science*, *100*, 4689–4696.

Tadros, T., Izquierd, P., Esquen, J., & Solans, C. (2004). Formation and stability of nano-emulsions. *Advances in Colloid and Interface Science*, *108–109*, 303–318.

Zetasizer Nano Series User Manual. (2004). *MAN0317, Issue 1.1*.

Zhao, Y., Wang, C. G., Chowb, A. H. L., Ren, K., Gong, T., Zhang, Z. R., et al. (2010). Self-nanoemulsifying drug delivery system (SNEDDS) for oral delivery of zedoary essential oil: Formulation and bioavailability studies. *International Journal of Pharmaceutics*, *383*, 170–177.